

Evolution of the microstructure of disperse Zinc-oxide during tribophysical activation

M. G. KAKAZEY, V. A. MELNIKOVA, T. SRECKOVIC*, T. V. TOMILA,
M. M. RISTIC*

Institute for the Problems of Material Science of the National Academy of Sciences of the Ukraine, Kyiv, Ukraine

**Joint Laboratory for Advanced Materials of the Serbian Academy of Sciences and Art, Belgrade, Yugoslavia*

E-mail: dep8@ipms.kiev.ua

The process of macro- and microstructural transformations of zinc-oxide powders, which were tribophysically activated by grinding in a vibro-mill was investigated using methods of transmission electron microscopy, infrared spectroscopy and X-ray. It is shown that tribophysical activation contributes to a gradual modification of the fine defect structure of zinc-oxide powders. In the starting stage agglomerates and bigger, longer particles are destroyed first of all. As a result of the formation of both volume and surface defects and changes of the character of interparticles interactions the plate-like polycrystal particles are created. They actually present sets of coherent scattering region. © 1999 Kluwer Academic Publishers

1. Introduction

For obtaining of optimal properties of both materials and products, a very careful control of changes of primarily morphological, microstructural and other characteristics is necessary. This is the reason why the investigation of the process of tribophysical activation, which is very often used in powder technology, is of both scientifically and practically interest [1, 2].

The problem of the evolution of the disperse zinc-oxide powders was investigated using methods of dispersion analysis and scanning electron microscopy (SEM) [3]. The powders were tribophysically activated by mechanical treatment—grinding in a vibro-mill. The evolution of the formed structures and decomposition-activation processes were not investigated in more detail earlier because of the limitations of the applied methods if analyzing particles had the dimensions $d \leq 1.0 \mu\text{m}$. So, for example, in samples of zinc-oxide powders, which were tribophysically activated for 3 min, the formation of oval forms was noticed, while the fragments of destruction of starting particles were not observed using the SEM method [3]. In this paper an assumption was made on the complex character of such structures which were formed from destroyed pieces of starting particles due to the influence of autohesion forces. The dynamics changes of different paramagnetic centers depending on the mechanical treatment time are observed in work [4]. It was interesting to find out the details of picture of the evolution of the microstructure of zinc-oxide powders during tribophysical activation using methods transmission electron microscopy (TEM), infrared spectroscopy (IR) and X-ray possessing the more high resolution. Some papers [5–8]

are devoted the research of synthesized zinc-oxide powders with use of these methods. The possibilities of IR are worthy of the special attention under analysis of zinc-oxide powders morphological changes. It follows from the purely phonon theory, known as the Theory of the Average Dielectric Constants (TADC). This theory was generalized by Hayashi *et al.* [9] for the case of randomly oriented ellipsoid particles having the anisotropic dielectric properties. In this theory, changes of particle form are considered from the viewpoint of ellipsoid parameters changes and are characterized by depolarization factors L_{\parallel} and L_{\perp} . Their values are equal for cylindrical particles 0 and 0.5, for spherical 0.33 and 0.33, and for plate-like 1 and 0 respectively [5, 9]. The TADC theory also enables to investigate the agglomerated powder states [8, 10] being a very suitable method for the analysis of the powder morphology.

2. Experiment

A commercial zinc-oxide powder with a purity of 99.96% and specific surface $S_p \approx 3.6 \text{ m}^2/\text{g}$ was used. The zinc-oxide powder was tribophysically activated by grinding in a vibro-mill (Tur MH 954/3 KXD HUMBOLDT NEDAG AG) in air from 3 up to 300 min.

The methods of transmission electron microscopy (JEM-IOOCX), infrared spectroscopy (Specord-M80) and X-ray diffraction (DRON-3) were used in these investigations.

For electron microscope the samples were prepared in the following way: the powders were dispersed in alcohol by ultrasound, and the obtained suspension were deposited by a thin layer on the (100) plane of a NaCl

monocrystal. After the alcohol evaporation a carbon layer was deposited on this surface under vacuum. Then the NaCl base was dissolved in water and the carbon films with zinc-oxide particles obtained by this way were used as working samples.

For infrared spectroscopy the zinc-oxide and KBr powders were carefully mixed in the ratio 1 : 300 and the obtained mixture was pressed into transparent rectangular plates with dimensions $5 \times 26 \text{ mm}^2$.

X-ray diffraction lines were obtained with using of a X-ray powder diffractometer with $\text{CuK}\alpha$ -radiation. These data were used for determination of the change in distances d between certain crystallographic planes (300) and (006), average sizes D of coherent-scattering region (CSR), microstrains e , minimal dislocation density ρ_D , dislocation density due to microstrain ρ_ξ and real dislocation density ρ_R .

3. Experimental results and discussion

3.1. Transmission electron microscopy

The morphology, dispersivity and defective structure of particles and agglomerates of zinc-oxide powders in different stages of tribophysical activation were investigated by transmission electron microscopy using the method of light and dark fields and microdiffraction. The such TEM micrograph shown the powder structure is accompanied by electron-diffraction photograph obtained from regions $0.5 \mu\text{m}$ in diameter that was cutted by an selective electron diaphragm (Fig. 1). Based on these results, one can conclude that the starting, unactivated zinc-oxide powder consists of microcrystal particles with dimensions from 0.1 to $1 \mu\text{m}$ and by high level of shape anisotropy. The cross-section of the microcrystal has a rectangular shape with clear expressed crystallographic planes and rounded two-facet angles (Fig. 1a—the starting powder, $\tau = 0$ min). Particles with a cylindrical shape can also be noticed. The anisotropy of particle shapes changes from equiaxial to needle-like with the ratio $d/1$ from 1 up to 0.1 . Joining together of two or more crystals with clearly expressed boundaries between grains can also be noticed. Electron diffraction patterns of individual particles present a regular network of single crystal reflections.

A three-minute's activation leads to the breaking-up primarily needlelike particles and large concretions (Fig. 1a, $\tau = 3$ min). In this activation stage, individual dislocations and dislocation loops appear in the structure of some single crystal particles.

A further continuation of activation (up to 30 min) trend of the increase of the number of small particles in the powder and their tendency to agglomerate continues. The boundaries of particles become indistinct (Fig. 1a, $\tau = 30$ min) and the increase of the level of particle defective structure (the dislocation density increases to 10^9 cm^{-2}) is noticed. The electron-diffraction photographs correspond to the set of reflections which originate from several single crystals.

After activation for 300 min a powder is a highly disperse mixture of small particles (Fig. 1a, $\tau = 300$ min). Most of these particles are in the form of aggregates with dimensions 0.3 – $0.1 \mu\text{m}$. The ring-like electron-

diffraction photographs indicate that these aggregates have a polycrystal structure. The regions with dimension of $d \sim 0.04 \mu\text{m}$ (by dark-field microscopy data) form such reflections. The high density of interfaces and defects does not enable to observe the high-angles boundaries in aggregates. However on the base of obtained results can conclude that the tribophysical activation by grinding leads to the breaking-up of starting particles up to fragments, which are very disordered and present the coherent-scattering region. According to X-ray analysis the size of CSR in these samples is $D_{100} \approx 0.036 \mu\text{m}$ and $D_{001} \approx 0.048 \mu\text{m}$. The small difference between dimensions d and D enables us to conclude that the starting zinc-oxide powders break up up to individual particles that themselves are CSR. On the other hand, particles formed by this way due to tribophysical activation join into aggregates of various dimensions and forms.

3.2. Infrared spectroscopy

The obtained spectra of zinc-oxide powders using IR spectroscopy are given in Fig. 2. The TADC method was used for their interpretation. The theoretical and experimental basis for the applicability of this method for the analysis of ultradisperse particles of optically anisotropic materials is given in literature [5–12]. In accordance with this theory the contribution of the influence of the shapes of small particles and agglomerates on two perpendicular optical modes ($\nu_{T\parallel} = 377 \text{ cm}^{-1}$ and $\nu_{T\perp} = 406 \text{ cm}^{-1}$ determined from IR-reflection spectra [13] or $\nu_{T\parallel} = 380 \text{ cm}^{-1}$ and $\nu_{T\perp} = 413 \text{ cm}^{-1}$ from combination scattering spectra [14]) is considered through depolarization effects, in which form factors L_{\parallel} and L_{\perp} (L_{\parallel} is connected with the crystallographic axis c and $L_{\parallel} + 2L_{\perp} = 1$) appear and also the filling factor f , which presents part of the total sample volume (its values are from 0 to 1). It is believed that an individual particle has the shape of a rotation ellipsoid around axis c . A graph which illustrates the positions of absorption peaks and also the form of some typical spectra in dependence of particles shapes for the case when $f \approx 0.003$ is given in [9] and corresponds to a system of non-interacting particles. This graph is used in this paper to identify extremes of registered spectra for samples whose grinding time is $\tau \leq 30$ min (Table I). The accounting of influence of the filling factor f enables to take into consideration the interactions between particles in the sample and as a result to separate the case of a system with non-interacting individual particles when $f \rightarrow 0$ and aggregates when $f \rightarrow 1$ [8, 10]. The TADC theory enables the analysis of IR-spectra of aggregates with different geometries (particle chains; triplets...) [10]. In [8] the calculations results of the IR-absorption spectra forms of spherical particles for several values of f are given. This enables the graphical presentation of $\nu_{\text{max}} = F(f)$ (Fig. 3). The obtained dependence of ν_{max} and the number of maximums of values L and f , only emphasizes the complexity and difficulties that exist when working with real systems. These systems are most often characterized by a set of different states. The superposition of absorption

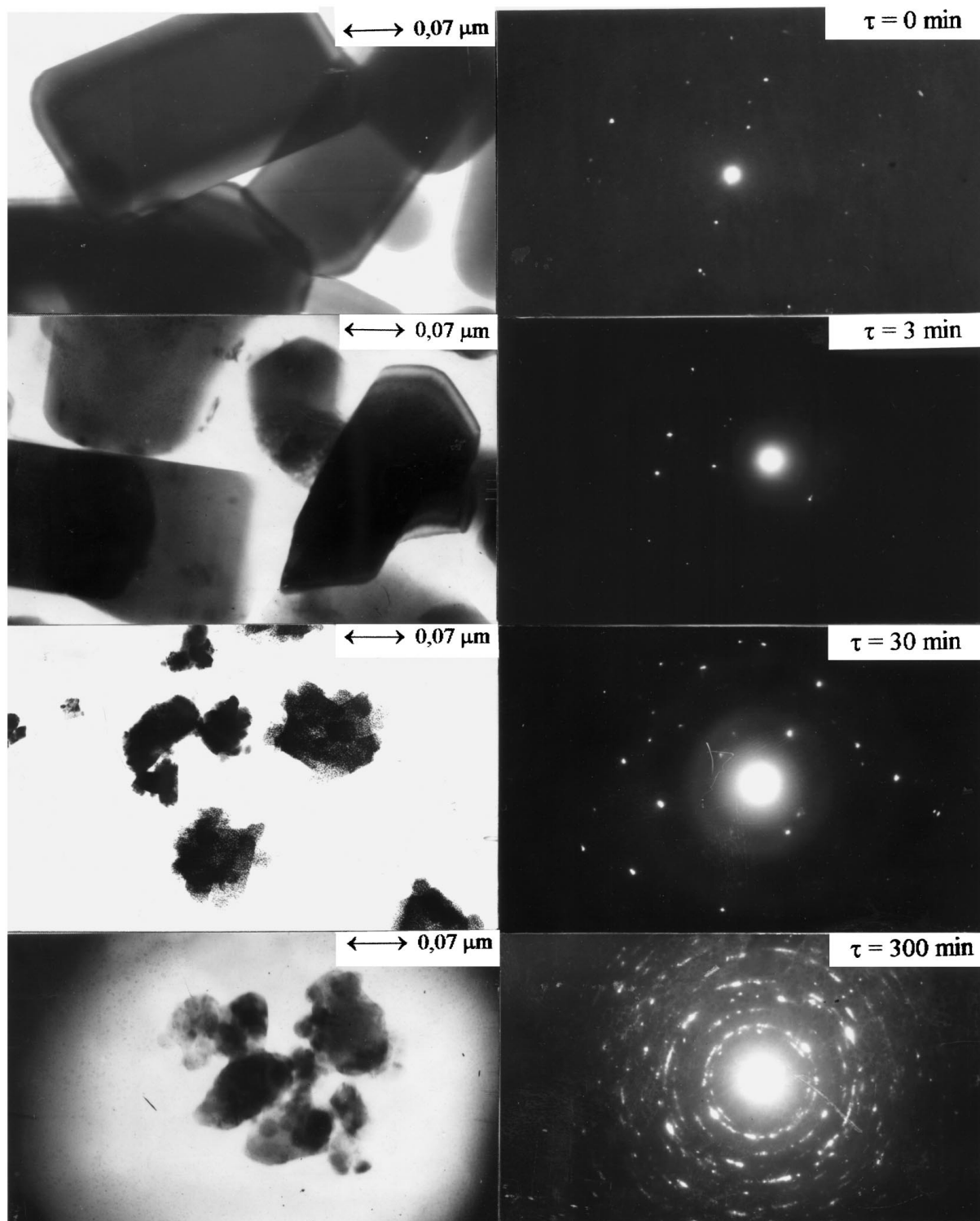


Figure 1 Electron micrographs (a) and electron diffraction patterns (b) of zinc-oxide powders at different stages of tribophysical activation.

zones of different origins in a narrow frequency range in which the spectra are registered (Fig. 2), makes their unique identification based only on IR analysis difficult.

The results of electron microscope investigations given earlier enable a classification of samples according to the character of particle interactions. Samples of zinc-oxide powder with $\tau \leq 30$ min are systems of non-interacting, individual particles, while in samples with $\tau > 30$ min, both individual particles and their agglomerates appear.

This analysis, which is in agreement with [9], enables the identification of registered absorption modes for

samples with grinding times from 0 to 30 min (Fig. 2) and also an estimation of parameters L_{\parallel} and L_{\perp} , which reflect the particles geometry (Table I). The modes with $\nu_1 = 535 \text{ cm}^{-1}$ and $\nu_3 = 488 \text{ cm}^{-1}$ are characterized for spectra of particles which have a dimension ratio along axis c and perpendicular to it $L_{\perp}/L_{\parallel} \approx 2$. The mode with $\nu_2 = 510 \text{ cm}^{-1}$ corresponds to particles with an almost equal axis (with $L_{\perp}/L_{\parallel} \approx 1$), while the mode with $\nu_4 = 435 \text{ cm}^{-1}$ corresponds to particles with a needle-like shape (with $L_{\perp}/L_{\parallel} \approx 3.5\text{--}4.5$). The appearance of modes ν_1, ν_2, ν_3 and ν_4 corresponds to the rising concentration of a corresponding particle shape in samples

TABLE I The position and identification of ν_{\max} in IR-spectra of tribophysically activated ZnO, values of depolarization factors L_{\perp} , L_{\parallel} and particle shape parameter L_{\perp}/L_{\parallel}

Sample	$\nu_1(\nu_{T\perp})$, cm^{-1}	$\nu_2(\nu_{T\parallel})$, cm^{-1}	$\nu_3(\nu_{T\parallel})$, cm^{-1}	$\nu_4(\nu_{T\parallel})$, cm^{-1}	L_{\parallel}	L_{\perp}	L_{\perp}/L_{\parallel}
Starting	537				0.22	0.39	1.7
$\tau = 0$ min		510			0.32	0.34	1
			488		0.20	0.40	2
$\tau = 3$ min				435	0.10	0.45	4.5
	540				0.20	0.40	2
		515			0.33	0.33	1
			490		0.20	0.40	2
$\tau = 30$ min				440	0.11	0.45	4
	537				0.22	0.39	1.7
		513			0.32	0.34	1
			485		0.20	0.40	2
			442	0.14	0.43	3	

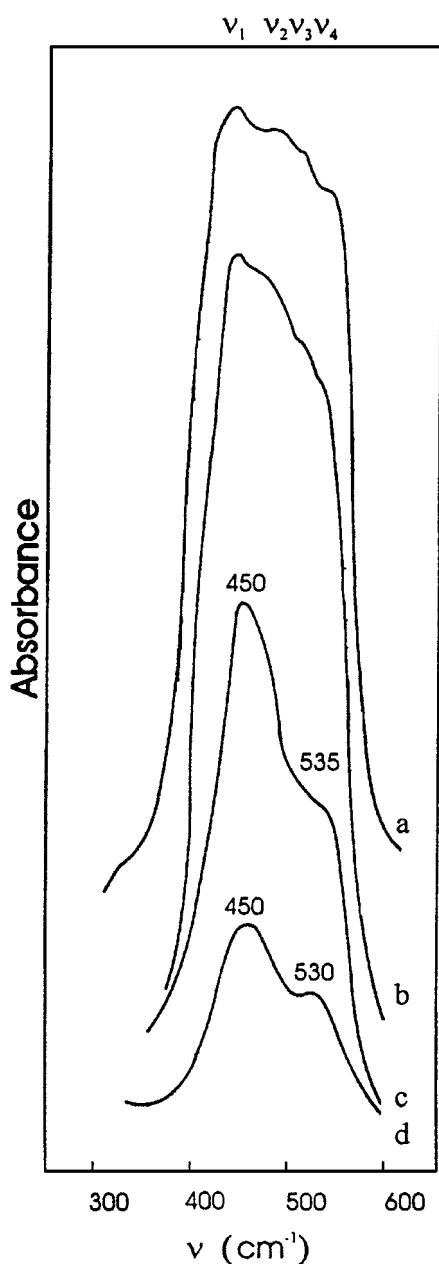


Figure 2 IR-spectra of zinc-oxide powders in KBr: (a) commercial sample; (b) activated 30 min; (c) activated 300 min; (d) activated 3 min and sintered at 950 °C for 30 min.

of zinc-oxide powder. An insignificant reduction of modes ν_1 , ν_3 and ν_4 and enlargement of mode ν_2 with the decrease of the grinding time up to 30 min (Fig. 2) indicates a decrease of the number of elongated and increase of the number of particles with equal axis. The decrease of the mode width at the semi-height $\Delta\nu_{3\min} \approx 170 \text{ cm}^{-1}$ and $\Delta\nu_{30\min} \approx 150 \text{ cm}^{-1}$ indicates on the narrowing of under the form of particles with the increase of τ .

A further prolongation of the activation time τ modifies the IR spectra, thus, that maximums which are characteristic for a system of non-interacting particles disappear, intensities are generally reduced and two fairly wide modes with $\nu = 535 \text{ cm}^{-1}$ and $\nu = 450 \text{ cm}^{-1}$ (Fig. 2, curve c) are appeared. These changes are the consequence of collective processes which occur after tribophysical activation for a long time—the agglomeration process. One can conclude that the mode with $\nu = 450 \text{ cm}^{-1}$ originates from agglomerates of particles with almost equal axis. The filling coefficient of these agglomerates can be estimates from Fig. 3 to be $f \approx 0.64$. The existence of a mode with $\nu = 535 \text{ cm}^{-1}$, in accordance with [7], points to the presence of plate-like agglomerates with the thickness/length (width) ratio from 0.3 to 0.5. A similar character of the modification of IR spectra is noticed but in sintered zinc-oxide samples with $\tau \leq 30$ min (Fig. 2, curve d).

3.3. X-ray

Having in mind, that the investigated zinc-oxide has a hexagonal crystal structure and that TEM analysis has established the anisotropy of particle forms, the characteristic microstructure parameters have been determined in two crystallographic directions: in the direction [100] (direction lying in the base plane) and the perpendicular direction [001]. The constant value of the integral intensity of diffraction lines (in the limits of measurement accuracy) permits to use the width of diffraction lines (B) for determination of average values of the crystallite sizes D_{100} , D_{001} and microstrains e_{100} and e_{001} . This procedure was fulfilled with application of the approximation method [15]. Accordingly changes in the width of diffraction lines from planes (100), (300) and (002), (006) were analyzed. As an standard a source zinc-oxide powder was used, as it

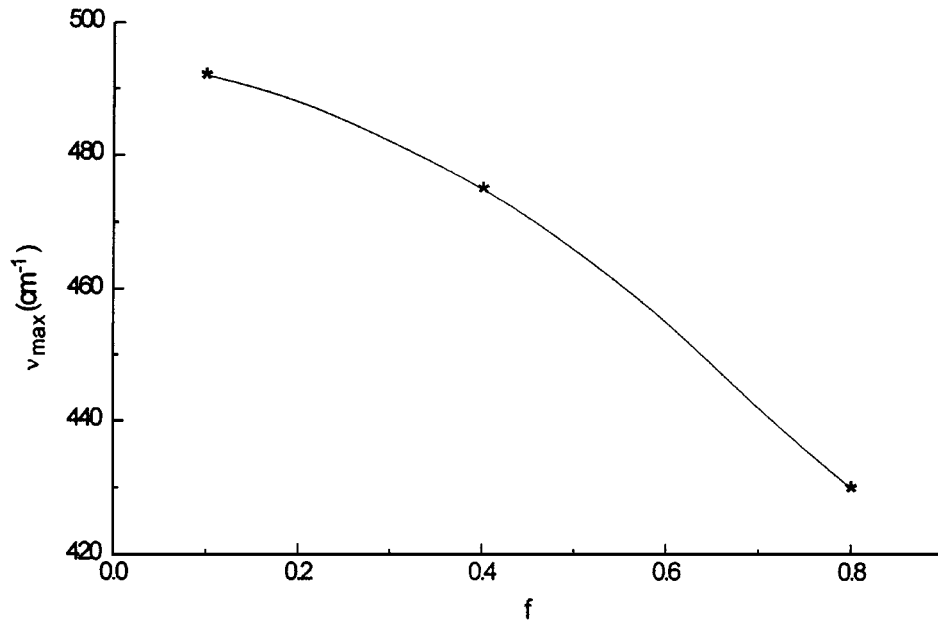


Figure 3 The dependence of the position of the IR-absorption peak for spherical particles as function of the filling factor f ; * denote the points calculated using [8].

has the well separated $K_{\alpha 1, \alpha 2}$ doublets. According to data given in [16] the growth axis of such crystallites is usually parallel to the c axis. In accordance with the facts stated above, the source zinc-oxide powder can be considered on average as a assemblage of approximately similar monocrystalline particles with dimensions: $0.2 \mu\text{m}$ in cross-section and $0.4 \mu\text{m}$ in length. The values of full width at a half maximum of diffraction lines of the standard (b_0), i.e. instrumental diffraction line widths, were corrected in accordance with these data and they were defined as CSR dimensions, i.e. crystallites: $D_{100} = 0.2 \mu\text{m}$ and $D_{001} = 0.4 \mu\text{m}$. In Table II the values of average sizes of coherent-scattering region D and microstrains e calculated with using of the above defined method are given.

The values D and e were used for calculation of dislocation density ρ_D and ρ_ξ correspondingly by the

Williams-Smallman method [17]:

$$\rho_D = 3n/D^2 \quad (1)$$

where n is the number of dislocations per the CSR surface (at calculation n was assumed equal 1);

$$\rho_\xi = k \cdot \xi^2 / (F \cdot b^2) \quad (2)$$

where k is a coefficient that depends on mechanical properties of the crystal, its microstructure, and also on the type of distribution of displacement in it (its values are usually between 2 and 25, we assume $k = 15$), and b is the Burgers vector, that is equal to the smallest interatomic distance ($b = 0.197 \text{ nm}$). Based on the Williams-Smallman analysis of ρ_D and ρ_ξ values (Table II), it can be concluded that $n = F$, which

TABLE II Values of distances between corresponding crystallographic planes d , average sizes of coherent-scattering region D , width of diffraction lines due to the existence of microstrains ξ , microstrains e , minimal dislocation densities ρ_D , dislocation density due to microstrain ρ_ξ and real dislocation density ρ_R , and average distances between dislocations h

τ (min)	Crystall. direction	hkl	$d \cdot 10^{-8}$ (cm)	D (μm)	$\xi \cdot 10^{-3}$	$e \cdot 10^{-3}$	$\rho_D \cdot 10^{10}$ (cm^{-2})	$\rho_\xi \cdot 10^{10}$ (cm^{-2})	$\rho_R \cdot 10^{10}$ (cm^{-2})	$h \cdot 10^{-8}$ (cm)
0	[100]	100								
		300	0.938(6)	0.2	0.51	0.18	0.8	1.0	0.9	1667
	[001]	006	0.867(2)	0.4	0.46	0.17	0.2	0.8	0.4	1875
3	[100]	100								
		300	0.938(5)	0.179	0.75	0.22	0.9	2.2	1.4	1197
	[001]	006	0.867(4)	0.347	0.53	0.18	0.3	1.1	0.6	1441
30	[100]	100								
		300	0.937(9)	0.098	1.25	0.28	3.1	6.0	4.3	712
	[001]	006	0.867(6)	0.152	0.83	0.23	1.3	2.7	1.9	1039
300	[100]	100								
		300	0.937(2)	0.036	3.64	0.48	23.1	51.2	34.4	242
	[001]	006	0.867(9)	0.048	2.32	0.38	13.0	20.8	16.4	381

implies the process of dislocation networks, so the real dislocation density can be determined using the expression:

$$\rho_R = (\rho_D \cdot \rho_\xi)^{1/2}. \quad (3)$$

The obtained results (Table II) show the reduction of D_{100} and D_{001} values and increase of microstrain ϵ with the increase of activation time, that is accompanied by a linear growth of the real dislocation density ρ_R . Observations of the D_{100}/D_{001} ratio, which characterizes the form changes of CSR, show that this ratio increases from 0.5 ($\tau = 0\text{--}30$ min) up to 0.75 ($\tau = 300$ min). Analysis of results given in Table II also clearly shows the tendency of a small reduction of the interplane distance between planes (300) and increase of the interplane distance between planes (006), which indicates a reduction of the lattice parameter a and increase of the lattice parameter c .

Decrease of the unit cell parameter a and increase of the parameter c with the increase of activation time τ is due to the formation of vacancy centers in the zinc-oxide lattice. According to EPR investigations of TA zinc-oxide powder [4] the following centers appear: (a) the complex zinc vacancy—interstitial zinc atom; (b) zinc vacancy (interstitial zinc atom localized at distances higher than a third coordination sphere); (c) divacancy zinc complex, localized in one plane (001); (d) oxygen vacancy. The formation of such centers in the wurtzite structure of zinc-oxide can be explained by removing of Zn^{2+} ions (O^{2-}) from the metal sublattice (oxygen) into interlayer space, that leads to the reduction of interatomic distances in the layers, i.e. reduction of parameter a , and the increase of parameter c .

There have been stated that CSR boundaries, formed during mechanical treatment of large crystals, are determined by the inhomogenous character of the localization of the admixture and other defects (dislocations and vacancies) in starting powders [18]. Many kinds of defect states suppose the existence of complex multi-level structure of their localization. This structure possesses the definite space periodicity in real materials. Tribophysical activation leads to gradual activation of this complex defect structure by further accumulation and generation of dislocations and vacancies. Having in mind all stated above, CSR evolution in differently activated zinc-oxide powders can be defined by the D_{100}/m and D_{001}/n ratios, where m and n are integers. Anal-

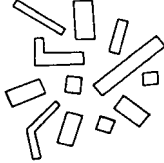

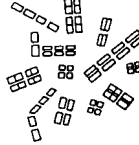

ysis of data given in Table II shows that $m \approx 2$ and $n \approx 3$ for powders activated for 30 min, while these values are $m \approx 6$ and $n \approx 9$ for powders activated for 300 min. Based on obtained values, it can be assumed that evolution of the CSR structure in particles during tribophysical activation of zinc-oxide powders has a discrete character.

4. Conclusion

The presented results allows to propose a general evolution scheme of the microstructure of disperse zinc-oxide during tribophysical activation. The starting, unactivated powder presents a set of individual particles and has a wide grain size ($d \supset [0.1 \mu\text{m}, 1 \mu\text{m}]$) and shape ($L_{\parallel}/L_{\perp} \supset [1, 10]$) distribution, though one can say that most particles have $L_{\parallel}/L_{\perp} \approx 1, 2$ and 4 and almost a single crystal structure. At the starting activation stage ($\tau \leq 30$ min) the existing concretions and longer particles break down, so the L_{\parallel}/L_{\perp} ratio decreases. The process of crumbling—deformation is accompanied by the appearance and development of a dislocation structure. The boundary surfaces of newly-formed particles have a complex geometrical form, i.e. they become bigger with the continuation of τ . So their role in the formation of stronger interparticle contacts due to the influence of autohesion forces [19] becomes more important. Such manner, at $\tau > 30$ min both processes of further breaking down and deformation and also autohesion processes in parallel are developed, that promotes a consolidation of newly-formed particles, but at qualitatively new level. The grinding process continues until the formation of individual particles with dimensions which correspond to the size of a single CSR. However due to autohesion interparticle interaction (due to the action of electrostatic forces, roughness and the expansion of the surface vacancy structure, intensifying of mechanothermal processes especially with prolonged tribophysical activation, the formation of a surface layer due to the interaction of zinc-oxide and grinding products from the mill and balls and the working environment) these particles consolidate into polycrystal agglomerates whose hardness and shape depend on the tribophysical activation conditions.

It is notified the direct connection between the filling coefficient f and agglomerate porosity Θ : $\Theta = (1 - f) \cdot 100\%$. So the process of the formation of plate-like polycrystal forms can be considered quite natural

TABLE III Scheme of the evolution of the microstructure of zinc-oxide powders during tribophysical activation

Samples				
Process	—	Breaking-up	Breaking-up, deformation, defect formation	Breaking-up, deformation, defect formation
Autohesion forces	Mechanical	Electrical	Electrical	Cohesion interaction, molecular, mechanical

as the result of the grinding—pressing process due to the action of mill balls during tribophysical activation and (partly) of such products when the external actions change again.

The proposed scheme of the evolution of the microstructure of zinc-oxide powder during tribophysical activation is corresponded in Table III.

5. Acknowledgment

This work was performed as part of the project “Prognosis of materials properties” financed by the Ministry for Science and Technology of Serbia, and also the cooperation of the Serbian Academy of Sciences and Arts and the Institute for the Problems of Material Science of the National Academy of Science of the Ukraine on the project “Physico-chemical processes of the formation and evolution of the structure of inorganic materials.” The authors would like to thank these institutions for all enabled research conditions.

References

1. YE. G. AWAKUMOV, “Mechanical Methods of the Activation of Chemical Processes” (Nauka, Novosibirsk, 1986, in Russian) p. 305.
2. G. HEINKE, “Tribochemistry” (Mir, Moskva, 1987, in Russian), p. 582.
3. T. SRECKOVIC, N. G. KAKAZEY and T. B. NOVAKOVIC, *Sci. Sintering* **27** (1995) 183.
4. N. G. KAKAZEY, T. V. SRECKOVIC and M. M. RISTIC, *J. Mater. Sci.* **32** (1997) 4619.
5. C. J. SERNA and J. E. IGLESIAS, *J. Phys. C* **20** (1987) 472.
6. M. ANDRES-VERGES and C. J. SERNA, *J. Mater. Sci. Lett.* **20** (1988) 970.
7. M. ANDRES-VERGES, A. MIFSUD and C. J. SERNA, *ibid.* **8** (1989) 115.
8. M. ANDRES-VERGES and M. MARTINEZ-GALLEGO, *J. Mater. Sci.* **27** (1992) 1756.
9. S. HAYASHI, N. NAKAMORI and H. KANAMORI, *J. Phys. Soc. Japan* **46** (1979) 176.
10. P. CIPE and R. ERVARD, *Phys. Rev. B* **14** (1971) 1715.
11. L. GENZEL and T. P. MARTIN, *Phys. Stat. Sol.* **51b** (1972) 91.
12. *Idem. Surface Sci.* **34** (1973) 33.
13. E. C. HELTEMES and H. L. SWINNEY, *J. Appl. Phys.* **38** (1967) 2387.
14. C. A. ARGUELLO, D. L. ROUSSEAU and S. R. S. PORTO, *Phys. Rev.* **181** (1969) 1351.
15. S. S. GORELIK and L. N. RASTORGUEV, “X-ray and Electron Diffraction Analysis of Metals” (Gostekhizdat, Moscow, 1963, in Russian).
16. F. HEILAND, G. MOLLARO and E. STOCKMANN, in “Solid State Physics,” Vol. 8, edited by F. Seitz and N. Y. Turnbull (Academic Press, London, 1959) p. 191.
17. G. WILLIAMSON and R. SMALLMAN, *Phil. Mag.* **1** (1956) 54.
18. N. G. KAKAZEY, D.Sc. Dissertation Abstract, Riga, 1991 (in Russian).
19. A. D. ZIMON and E. L. ANDRIANOV, “Autohesia Loose Materials” (Metallurgiya, Moscow, 1978, in Russian) p. 288.

Received 15 August 1996
and accepted 6 October 1998